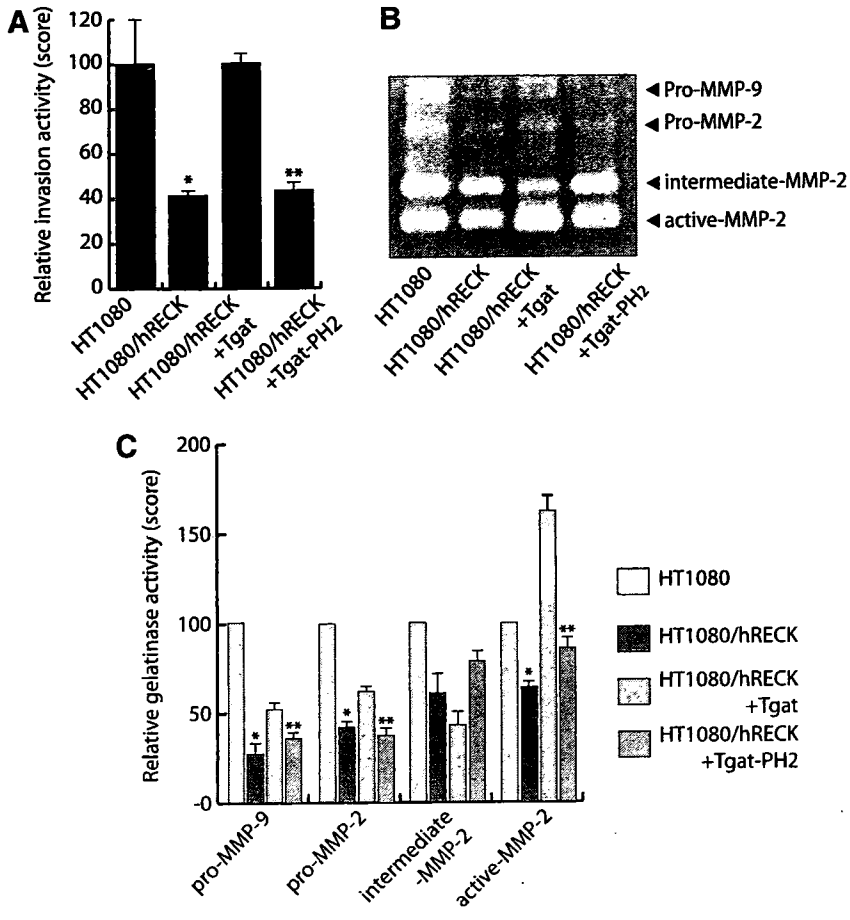

Fig. 4. Function of RECK is inhibited by the expression of Tgat through its C-terminal region. (A) Relative invasion activities. The migrated cells were stained and then counted under light microscopy. Average migrated cell numbers of HT1080 is determined as score 100 and invasive activities of indicated are expressed as relative scores. *, HT1080 and HT1080/RECK ($P < 0.01$); **HT1080/RECK and HT1080/hRECK+Tgat ($P < 0.01$). (B) Gelatin zymogram with the conditioned media from HT1080 and indicted transformants. (C) Relative gelatinase activities. *HT1080 and HT1080/RECK ($P < 0.01$); **HT1080/RECK and HT1080/hRECK+Tgat ($P < 0.01$).

human cDNAs inducing flat reversion of v-Ki-ras-transformed NIH3T3 cells [4–6]. The following studies have supported that RECK functions as a suppressor of angiogenesis and metastasis by inhibiting the MMPs activities. RECK is a glycoprotein with serine protease inhibitor-like domains and anchors the cell membrane through the C-terminal glycosylphosphatidylinositol moiety. RECK post-transcriptionally regulates the members of MMP family, MMP-2 and MMP-9, by various mechanism [7,8]. RECK inhibits not only the secretion of proMMP-9 from the cell but also the processing of proMMP-2 to its intermediate species, and the following autocatalysis to form activated MMP-2. Degradation of the extracellular matrix (ECM) by MMPs is a crucial step in tissue remodeling and tumor invasion and metastasis [9]. Depending on their substrate specificities, MMPs are broadly divided into collagenase, stomelysins, and gelatinase. MMP-2 (Gelatinase A) and MMP-9 (gelatinase B) degrade denatured collagens, native type IV and V collagens. MMP-2 and MMP-9 are potentially involved in carcinogenesis and malignant phenotypes of tumor cells, since correlation between their activity and the malignancy of tumors have been documented in a number of studies [10–13].

In the present study, we have found that Tgat certainly enhances the invasive potential of NIH3T3 cells in correlation with the enhanced secretion of activated MMP-2 and proMMP-9. In contrast, the expression of Tgat alone gave little effect on the invasion potential in human fibrosarcoma cell line HT1080, possessing highly invasive potential but lacking the expression of hRECK. Introduction of the hRECK expression, however, reduced the invasive potential of HT1080 by 60%, which was restored by co-expression of Tgat. Levels of activated MMP-2 were again well correlated with the invasion potential in HT1080 cells. We have previously found that a Tgat mutant lacking GEF activity, constructed by single-nucleotide substitution of Tgat cDNA corresponding GEF domain, did not show the invasive potential of NIH3T3 cells [1]. These results suggest that Tgat may block the function of RECK by physical association via the C-terminal unique sequence, resulting in activation of MMPs and enhancing the cell invasion.

Accumulating evidence has suggested that the altered expression of RECK plays a role in various human malignancies. Expression levels of RECK were lower in breast cancer [14], or hilar cholangiocarcinoma [15] than in adjacent normal tissue specimens. On the other hand, the patients with hepatic cell carcinoma with high RECK expression tended to show better survival and such tumor were less invasive [16]. Tgat was originally identified in a cDNA library derived from fresh ATL cells [1]. The Tgat mRNA was detectable in ATL cells and tissues, in contrast to the undetectable level in normal lymphocytes, suggesting some roles of Tgat in the malignant phenotype of ATL [1]. Acute ATL progresses rapidly and the median survival after diagnosis is approximately six months [17]. The highly potent invasiveness of ATL tumor cells into various organs has been recognized to be a factor affecting the poor prognosis. A significant elevation of plasma MMP-9 was shown to be detected in some ATL patients, particularly in the patients with malignant cell infiltration [18,19]. Tax, an oncoprotein encoded by HTLV-1, is not only trans-activator of the viral transcription but also responsible for trans-activation or trans-repression of a variety of cellular genes coding cytokines and regulators of cell cycles, DNA repair or apoptosis. Tax has been shown to trans-activate the MMP-9 gene, however, Tax is hardly implicated to the enhanced the MMP activity observed in ATL cells since Tax expression is usually undetectable in fresh ATL cells. Although we have not clarified the expression of RECK in ATL cells, yet it is conceivable that Tgat expression in ATL cells may function as an enhancer of MMP activities via the direct interaction with RECK and cause the invasive phenotype. An agent that blocks the physical interaction between Tgat and RECK could be beneficial in therapy of ATL, although the mechanisms of Tax-independent MMPs activation in ATL cells should be investigated more extensively.

Acknowledgments

This work was supported by grants from the Ministry of Education, Culture, Sports, Science and Technology of Japan to R.M.

Appendix A. Supplementary data

Supplementary data associated with this article can be found, in the online version, at doi:10.1016/j.bbrc.2007.02.051.

References

[1] N. Yoshizuka, R. Moriuchi, T. Mori, K. Yamada, S. Hasegawa, T. Maeda, T. Shimada, Y. Yamada, S. Kamihira, M. Tomonaga, S. Katamine, An alternative transcript derived from the trio locus encodes a guanosine nucleotide exchange factor with mouse cell-transforming potential, J. Biol. Chem. 279 (2004) 43998–44004.

[2] I.P. Whitehead, S. Campbell, K.L. Rossman, C.J. Der, Dbl family proteins, Biochim. Biophys. Acta 1332 (1997) F1–F23.

[3] A. Hall, Rho GTPases and the actin cytoskeleton, Science 279 (1998) 509–514.

[4] M. Noda, H. Kitayama, T. Matsuzaki, Y. Sugimoto, H. Okayama, R.H. Bassin, Y. Ikawa, Detection of genes with a potential for suppressing the transformed phenotype associated with activated ras genes, Proc. Natl. Acad. Sci. USA 86 (1989) 162–166.

[5] H. Kitayama, Y. Sugimoto, T. Matsuzaki, Y. Ikawa, M. Noda, A ras-related gene with transformation suppressor activity, Cell 56 (1989) 77–84.

[6] C. Takahashi, N. Akiyama, T. Matsuzaki, S. Takai, H. Kitayama, M. Noda, Characterization of a human MSX-2 cDNA and its fragment isolated as a transformation suppressor gene against v-Ki-ras oncogene, Oncogene 12 (1996) 2137–2146.

[7] C. Takahashi, Z. Sheng, T.P. Horan, H. Kitayama, M. Maki, K. Hitomi, Y. Kitaura, S. Takai, R.M. Sasahara, A. Horimoto, Y. Ikawa, B.J. Ratzkin, T. Arakawa, M. Noda, Regulation of matrix metalloproteinase-9 and inhibition of tumor invasion by the membrane-anchored glycoprotein RECK, Proc. Natl. Acad. Sci. USA 95 (1998) 13221–13226.

[8] J. Oh, R. Takahashi, S. Kondo, A. Mizoguchi, E. Adachi, R.M. Sasahara, S. Nishimura, Y. Imamura, H. Kitayama, D.B. Alexander, C. Ide, T.P. Horan, T. Arakawa, H. Yoshida, S. Nishikawa, Y. Itoh, M. Seiki, S. Itohara, C. Takahashi, M. Noda, The membrane-anchored MMP inhibitor RECK is a key regulator of extracellular matrix integrity and angiogenesis, Cell 107 (2001) 789–800.

[9] L.A. Liotta, P.S. Steeg, W.G. Stetler-Stevenson, Cancer metastasis and angiogenesis: an imbalance of positive and negative regulation, Cell 64 (1991) 327–336.

[10] B. Davies, J. Waxman, H. Wasan, P. Abel, G. Williams, T. Krausz, D. Neal, D. Thomas, A. Hanby, F. Balkwill, Levels of matrix metalloproteases in bladder cancer correlate with tumor grade and invasion, Cancer Res. 53 (1993) 5365–5369.

[11] M. Yamamoto, S. Mohanam, R. Sawaya, G.N. Fuller, M. Seiki, H. Sato, Z.L. Gokaslan, L.A. Liotta, G.L. Nicolson, J.S. Rao, Differential expression of membrane-type matrix metalloproteinase and its correlation with gelatinase A activation in human malignant brain tumors in vivo and in vitro, Cancer Res. 56 (1996) 384–392.

[12] V.M. Kahari, U. Saarialho-Kere, Matrix metalloproteinases and their inhibitors in tumour growth and invasion, Ann. Med. 31 (1999) 34–45.

[13] L.M. Coussens, C.L. Tinkle, D. Hanahan, Z. Werb, MMP-9 supplied by bone marrow-derived cells contributes to skin carcinogenesis, Cell 103 (2000) 481–490.

[14] P.N. Span, C.G. Sweep, P. Manders, L.V. Beex, D. Leppert, R.L. Lindberg, Matrix metalloproteinase inhibitor reversion-inducing cysteine-rich protein with Kazal motifs: a prognostic marker for good clinical outcome in human breast carcinoma, Cancer 97 (2003) 2710–2715.

[15] Y. Li, Y. Zhang, Q. Zheng, Expression of RECK gene and MMP-9 in hilar cholangiocarcinoma and its clinical significance, J. Huazhong. Univ. Sci. Technol. Med. Sci. 25 (2005) 552–554.

[16] K. Furumoto, S. Arii, A. Mori, H. Furuyama, M.J. Gorrin Rivas, T. Nakao, N. Isobe, T. Murata, C. Takahashi, M. Noda, M. Imamura, RECK gene expression in hepatocellular carcinoma: correlation with invasion-related clinicopathological factors and its clinical significance. Reverse-inducing-cysteine-rich protein with Kazal motifs, Hepatology 33 (2001) 189–195.

[17] M. Shimoyama, K. Ota, M. Kikuchi, K. Yunoki, S. Konda, K. Takatsuki, M. Ichimaru, M. Ogawa, I. Kimura, S. Tominaga, et al., Chemotherapeutic results and prognostic factors of patients with advanced non-Hodgkin's lymphoma treated with VEPA or VEPA-M, J. Clin. Oncol. 6 (1988) 128–141.

[18] T. Hayashibara, Y. Yamada, Y. Onimaru, C. Tsutsumi, S. Nakayama, N. Mori, T. Miyanishi, S. Kamihira, M. Tomonaga, T. Maita, Matrix metalloproteinase-9 and vascular endothelial growth factor: a

possible link in adult T-cell leukaemia cell invasion, Br. J. Haematol. 116 (2002) 94–102.
[19] N. Mori, H. Sato, T. Hayashibara, M. Senba, T. Hayashi, Y. Yamada, S. Kamihira, S. Ikeda, Y. Yamasaki, S. Morikawa, M. Tomonaga, R. Geleziunas, N. Yamamoto, Human T-cell leukemia virus type I Tax transactivates the matrix metalloproteinase-9 gene: potential role in mediating adult T-cell leukemia invasiveness, Blood 99 (2002) 1341–1349.

プリオン病

新　竜一郎

長崎大学大学院医歯薬学総合研究科助教

片峰　　茂

長崎大学大学院医歯薬学総合研究科教授

保健の科学　第49巻　第10号（2007.10）別刷

0018-3342/07/¥250/論文/JCLS　保健の科学　第49巻　第10号　2007年

特集　新興・再興感染症の現状と予防

プリオン病

新　竜一郎[1)]，片峰　茂[2)]

1. プリオン病とは

プリオン病（伝達性海綿状脳症）は，感染病原体プリオンによって引き起こされる致死性の神経変性疾患であり，ヒトのクロイツフェルトヤコブ病（Creutzfeldt-Jakob disease：CJD），ヒツジのスクレイピー，牛の牛海綿状脳症（Bovine Spongiform encephalopathy: BSE）などが代表的な疾患である．感染病原体プリオンは，ウイルス，細菌などとは異なり病原特異的な核酸をもたず，おそらくは単一のタンパク質（異常型プリオンタンパク）のみから構成されているとするタンパク単独仮説（protein-only hypothesis）が提唱され，それを支持する多くの実験結果の集積と共に，広く受け入れられるようになった．つまり，プリオンとはこの疾患の病原体に与えられた名前であり，その主要構成因子が異常型プリオンタンパクである（時に異常プリオンという表現がマスコミ等で用いられることがあるが，これは両者を混同した間違った用語）．異常型プリオンタンパクは，ほ乳類の主に神経系に発現している正常型プリオンタンパクが構造上変化したもので，正常型に比べ，ベータシート含量が非常に高く，そのため，①凝集しやすく不溶性，②タンパク分解酵素処理に抵抗性，③通常の滅菌方法では完全に不活化できない，④アミロイド斑を形成することもある，などの性質をもつ．BSEの病原体は他のプリオン病に比べ，さらに耐熱性が高いことが知られており，そのため汚染された肉骨粉を通じてBSEの流行が起きてしまったと考えられる．

2. プリオン病発生のメカニズム

正常型から異常型への変換が起こる原因として，第1にプリオン感染組織等の汚染により，外部から生体内に侵入した異常型が正常型を次々に自分自身と同じ構造に変換するというメカニズムが挙げられる（感染性プリオン病）．第2に，生体内で正常型プリオンタンパクが非常に低い確率ながら自然発生的に，異常型プリオンタンパクへと変化し，それが変換反応の種となって第1のメカニズムと同様，正常型から異常型への変換反応が進行するというものである（孤発性プリオン病）．第3に，プリオンタンパク遺伝子の変異により正常型が構造異常を起こしやすくなり，異常型プリオンタンパクが形成され，プリオン病発病に至ると考えられる遺伝性プリオン病がある．ヒトのCJDでは，孤発性が約80～90％を占め，遺伝性が10～15％程度の頻度で発生し，残りが感染性である．今特集の観点から主に感染性CJD，

筆者：1）あたらし　りゅういちろう（長崎大学大学院医歯薬学総合研究科助教）
2）かたみね　しげる（長崎大学大学院医歯薬学総合研究科教授）

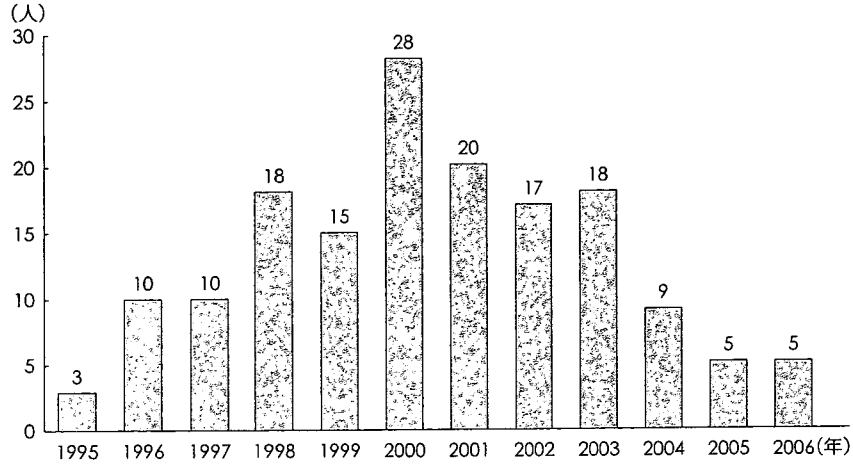

図1 イギリスでの変異型CJDによる年次別死亡者数
(The Univer sity of Edinburgh, 2007,[5])

特に変異型CJDの現況と今後の予防，対策に重点をおいて述べる．BSEの現況とこれまでの対策については，文献1, 2を参照していただきたい．

3. 変異型CJD

1996年，BSE発症牛からの感染が原因と強く推測される変異型CJDがイギリスで報告され，世界中に大きな衝撃を与えた．変異型CJDと孤発性CJDは臨床経過や病理像が異なるのみならず，60歳代が発症のピークである孤発性に対し，変異型では平均発症年齢が27歳と若いことが特徴のひとつである．変異型CJDの2006年2月までの集計ではイギリスで160例，その他の国で計28症例（フランス16例，アイルランド3例，アメリカ2例，カナダ，イタリア，日本，オランダ，ポルトガル，サウジアラビア，スペインで1例）が報告されている．アイルランドの1例，アメリカの2例，カナダ，日本の各1例はイギリスでの滞在時に感染したと考えられている[3,4]．イギリスでの変異型CJDによる年次別死亡者数を図1[5]に示す．

4. 種の壁：species barrier

イギリスでのBSE牛は正式に報告されただけでも18万頭以上であり，おそらくは数十万頭以上ものBSE感染牛が1990年代初頭までに消費されたと考えられている．しかし，この莫大なBSE感染牛の消費量に対して，現在までの変異型CJD発症例は百数十例程度である．その理由のひとつに牛とヒトの間に“種の壁：species barrier”が存在することが挙げられる．一般的にプリオン病では接種側と受容側の動物が同種である場合，特にプリオンタンパクの配列が一致していた方が潜伏期は短く，異なる場合は長くなる傾向があり，発症しないことも多い．しかし，同一種に2回，3回と継代接種を続けると潜伏期は短くなり安定化することが知られている（順応化：adaptation）．プリオンタンパクのアミノ酸配列は種によって少しずつ異なり，また同一種内でも遺伝的多型性が存在する．このヒトと牛の間のプリオンタンパク配列の違いが，BSE牛からヒトへの感染に防御的な役割を果たした可能性が指摘されている．さらにヒトではアミノ酸129番目のメチオニン（Met）あるいはバリン（Val）の多型がよく知られ，プリオン病の潜伏期や病理像に影響する．この多型の割合は人種，民族によ

り大きく異なり，例えばイギリス人ではMet/Metタイプが38％，Met/Valが51％，Val/Valが12％であるのに対して[6]，日本人では90％以上がMet/Metタイプで Val/Valはほとんど存在しない[7]．変異型CJDではこれまで発病したすべての症例がMet/Metタイプであった点が非常に特徴的であった．ヒト以外のほ乳類ではこの部位に相当するアミノ酸はメチオニンであり，感染源と受容側のこのアミノ酸部位の相違がBSEに対する感受性の違いをもたらし，結果としてこれまでの変異型CJD症例のほとんどがMet/Metタイプであったと考えられる．種の壁以外にプリオン病の潜伏期に影響を与える因子として，感染経路による違いが挙げられる．動物実験では同一の接種量で比較すると，脳内接種がもっとも潜伏期が短く，腹腔内，経口接種の順となる．市場に出回ったBSE牛の大部分は感染効率の悪い経口摂取により消費されたと考えられ，そのこともこれまでの発症者数を少なくしている要因と思われる．

マカクサルやヒトプリオンタンパクトランスジェニック（Tg）マウスを用いた感染実験からも，牛とヒトの間の種の壁の存在を支持する結果が得られている．5gのBSE牛の脳乳剤を経口的に与えたマカクサル2匹のうち1匹のみが60カ月後に発症したのに対し（もう1匹は76カ月後も発症せず，扁桃の生検でも異常型プリオンタンパクは検出されなかった），変異型CJDに相当するBSE感染マカクサルの脳乳剤を同量与えた場合はそれぞれ44カ月，47カ月後に2匹とも発症した[8]．一方，ヒトプリオンタンパクTgマウスはBSE牛の脳乳剤を脳内接種しても600日以上観察しても発症せず，また異常型プリオンタンパクも検出されなかった．しかし変異型CJDを接種した場合，Met/MetのTgマウスは15匹中11匹が異常型プリオンタンパク陽性であり，Met/ValのTgマウスは，Met/MetのTgマウスよりも潜伏期は長かったが，ほとんどのマウス(11/13)に異常型プリオンタンパクの蓄積がみられた．Val/ValのTgマウスは，15匹中1匹にのみ異常型プリオンタンパクが検出された[9]．もしこれらの結果がヒトの実際の変異型CJD感受性を反映したものであるとすれば，BSEからの感染よりも変異型CJDからの感染がより容易に，より多くの人口に対して起こりうる可能性を示しているといえる．この二次感染の危険性は，すでに現実のものとなっている．実際，変異型CJDが血液を介して新たに二次感染したと考えられる症例が報告されている．これまでに献血時には未発症でその後発病した変異型CJD患者から66人もが輸血を受けており，その中から4例の新たな変異型CJD感染が引き起こされた[10,11]．その中の一例は神経症状を示さず，別の原因で死亡したものの，死後脾臓に異常型プリオンタンパクが検出され，Met/Valタイプであった[12]．また，66人中24人が生存中で変異型CJD発症の危険性に晒されている（39人はCJD以外の病気で死亡）．これら輸血感染の4例はすべて1996～1999年の間に白血球が除去されていない赤血球成分を輸血されている．イギリスでは1999年10月より輸血の際，白血球（血液成分の中で相対的に感染性が高いと考えられる）を除去した血液を使用するようになったが，この処置により変異型CJD感染の危険性を減らすことができるかどうかは確かではない[11]．また，現時点では輸血以外の経路での感染は報告されていないが，汚染された手術器具を介しての感染の可能性も指摘されている．

5. 変異型CJD潜伏感染者（キャリア）の存在

1950年代，パプア・ニューギニアのフォア族に，宗教的儀礼として認められた食人の慣習であるカニバリズムにより流行した感染性プリオン病であるクールー病では，ヒトからヒトへの同種内感染であるにもかかわらず，潜伏期は40年以上の症例もあることが判明している[6]．したがって，牛からヒトへの異種間感染である変異型CJDの場合では，種の壁を考慮すると，潜伏期はクールー病以上になることが予想される．また，プリオン病では，非常に少ない量のプリオンを感染させた

ときや種を越えての感染の場合，寿命内では発症しないが，異常型プリオンタンパクの蓄積が非常にゆっくりと進行するキャリア（潜伏感染）状態が起きることが動物実験からわかっていた．これらを考え合わせると，変異型CJDでも未発症の感染者やキャリアが多数存在する可能性が想定される．変異型CJDでは孤発性CJDと異なり虫垂，扁桃などのリンパ組織に異常型プリオンタンパクが高頻度に検出される．その性質を利用して，イギリスで1995～2000年に除去手術を受け，保存されていた組織12,674個（虫垂11,109個と扁桃1,565個）について検査が行なわれ，そのうち3個に異常型プリオンタンパクがみつかった．その結果から，イギリスには100万人に237例（95%信頼区間：49～692例／100万人）の変異型CJD感染者がいる可能性が示唆された[13]．この陽性であった3個の虫垂のうち2個のプリオンタンパクのコドン129多型を調べたところ，両者ともVal/Valタイプであった[14]．前述した輸血によるMet/Valタイプへの感染とも合わせると感受性は異なるものの，すべてのタイプが少なくとも変異型CJDキャリアになり得ることを示している．これらの未発症の感染者が今後発症するのか，あるいは未発症のままキャリアとして終わるのかどうかについて確かなことはわからないが，変異型CJDの二次感染を引き起こさないためには十分な感染予防対策が必要である．

6. 今後の課題

1990年代からのBSE対策によりBSEの数は激減した[3,4]．それと共に特定危険部位の除去やBSE検査の効果も加わり，BSE感染牛による新たな変異型CJD　感染も激減したと推測される．しかし，前述したようにそれ以前に感染してしまった変異型CJDキャリアはイギリスを中心に相当数存在することが予想されており，今後はヒトからヒトへの二次感染を防ぐことが非常に重要である．輸血による変異型CJD感染の可能性が指摘されて以降，イギリスでは輸血による感染を防ぐため，次のような対策が行なわれてきた[15]．

①1997年以降，変異型CJDの可能性のあるものも含め，すべての患者は登録され，献血歴がないかチェックされる．もし献血歴があれば，その血液はただちに除去され，すでに輸血を受けてしまった人に対してはその危険性を知らせる．

②凝固因子等の産生に用いられる血漿は，イギリス以外の国のものを用いる（1998年7月イギリス保健省発表）．

③1999年10月以降，輸血に用いられるすべての血液から白血球を除去する．

④1996年1月以降に生まれた子どもに用いられる新鮮凍結血漿はアメリカ合衆国製のものを用いる（2002年8月イギリス保健省発表）．2005年夏には16歳以下のすべての子どもにその使用が拡大された．

⑤イギリス国外に由来する血漿を長期確保するため，イギリス保健省はアメリカ合衆国最大の独立血漿収集業者であるLife Resources Incorporatedを2002年8月に買収した．

⑥2004年4月以降，イギリスで1980年以後，輸血を受けた人は血液ドナーになることはできない．2004年8月には輸血を受けたかどうかはっきりしない人も制限の対象になった．

⑦2005年後期以降，後に変異型CJDを発症した患者に血液を供給した経歴のある人は今後血液ドナーになることはできない．

これら以外のさらなる対策としては，血液や手術器具からプリオンを効果的に除去する方法や変異型CJDキャリアを発見するための発症前の診断法の開発と実施が早急に必要であろう．究極的には変異型CJDだけでなく，すべてのプリオン病に対する治療法の開発も強く望まれる．

文　献

1) 厚生労働省：「牛海綿状脳症（BSE）関係」ホームページ（Q&Aなど）．http://www.mhlw.go.jp/kinkyu/bse.html（2007年8月9日現在）
2) 徳島大学大学院ヘルスバイオサイエンス研究部附属動物実験施設：人獣共通感染症（Zoonoses）講義．　http://www.anex.med.tokushima-u.

ac.jp/topics/index.html (2007年8月9日現在)
3) Bradley R et al. : Variant CJD (vCJD) and bovine spongiform encephalopathy (BSE) : 10 and 20 years on : part 1. Folia Neuropathol, 44 (2) : 93-101, 2006.
4) Collee JG et al. : Variant CJD (vCJD) and bovine spongiform encephalopathy (BSE) : 10 and 20 years on : part 2. Folia Neuropathol, 44 (2) : 102-110, 2006.
5) The Univer sity of Edinburgh : CJD Statistics. 2007. http://www.cjd.ed.ac.uk/figures.htm (2007年8月9日現在)
6) Collinge J et al. : Kuru in the 21st century-an acquired human prion disease with very long incubation periods. Lancet, 367 (9528) : 2068-2074, 2006.
7) Ohkubo T et al. : Absence of association between codon 129/219 polymorphisms of the prion protein gene and Alzheimer's disease in Japan. Ann Neurol, 54 (4) : 553-554, 2003.
8) Lasmézas CI et at. : Risk of oral infection with bovine spongiform encephalopathy agent in primates. Lancet, 365 (9461) : 781-783, 2005.
9) Bishop MT et al. : Predicting susceptibility and incubation time of human-to-human transmission of vCJD. Lancet Neurol, 5 (5) : 393-398, 2006.
10) Wroe SJ et al. : Clinical presentation and pre-mortem diagnosis of variant Creutzfeldt-Jakob disease associated with blood transfusion : a case report. Lancet, 368 (9552) : 2061-2067, 2006.
11) Health Protection Report : Fourth case of transfusion-associated variant-CJD infection. Vol. 1 No. 3, 2007.
12) Peden AH et al : Preclinical vCJD after blood transfusion in a PRNP codon 129 heterozygous patient. Lancet, 364 (9433) : 527-529, 2004.
13) Hilton DA et al. : Prevalence of lymphoreticular prion protein accumulation in UK tissue samples. J Pathol, 203 (3) : 733-739, 2004.
14) Ironside JW et al. : VVariant Creutzfeldt-Jakob disease : prion protein genotype analysis of positive appendix tissue samples from a retrospective prevalence study. BMJ, 332 (7551) : 1186-1188, 2006.
15) Health Protection Agency : 4th case of variant CJD infection associated with blood transfusion. 2007. http://www.hpa.org.uk/hpa/news/articles/press_releases/2007/070118_vCJD.htm (2007年8月9日現在)

July 17, 2007 | vol. 104 | no. 29 | pp.11921-11926

PNAS

Proceedings of the National Academy of Sciences of the United States of America www.pnas.or

Hot spots in prion protein for pathogenic conversion

Kazuo Kuwata, Noriyuki Nishida, Tomoharu Matsumoto, Yuji O. Kamatari, Junji Hosokawa-Muto, Kota Kodama, Hironori K. Nakamura, Kiminori Kimura, Makoto Kawasaki, Yuka Takakura, Susumu Shirabe, Jiro Takata, Yasufumi Kataoka, and Shigeru Katamine

Hot spots in prion protein for pathogenic conversion

Kazuo Kuwata[†‡§], Noriyuki Nishida[¶], Tomoharu Matsumoto[†], Yuji O. Kamatari[†], Junji Hosokawa-Muto[†], Kota Kodama[†], Hironori K. Nakamura[†], Kiminori Kimura[†], Makoto Kawasaki[¶], Yuka Takakura[¶], Susumu Shirabe[‖], Jiro Takata[††], Yasufumi Kataoka[††], and Shigeru Katamine[¶]

[†]Center for Emerging Infectious Diseases, [‡]Department of Gene and Development, Graduate School of Medicine, Gifu University, 1-1 Yanagido, Gifu 501-1194, Japan; [¶]Department of Molecular Microbiology and Immunology, [‖]Internal Medicine I, Nagasaki University Graduate School of Biomedical Sciences, 1-12-4 Sakamoto, Nagasaki 852-8523, Japan; and [††]Department of Pharmaceutical Care and Health Sciences, Faculty of Pharmaceutical Sciences, Fukuoka University, 8-19-1 Nanakuma, Jyonann-ku, Fukuoka 814-0180, Japan

Edited by Stanley B. Prusiner, University of California, San Francisco, CA, and approved June 6, 2007 (received for review March 22, 2007)

Prion proteins are key molecules in transmissible spongiform encephalopathies (TSEs), but the precise mechanism of the conversion from the cellular form (PrP^C) to the scrapie form (PrP^{Sc}) is still unknown. Here we discovered a chemical chaperone to stabilize the PrP^C conformation and identified the hot spots to stop the pathogenic conversion. We conducted *in silico* screening to find compounds that fitted into a "pocket" created by residues undergoing the conformational rearrangements between the native and the sparsely populated high-energy states (PrP*) and that directly bind to those residues. Forty-four selected compounds were tested in a TSE-infected cell culture model, among which one, 2-pyrrolidin-1-yl-*N*-[4-[4-(2-pyrrolidin-1-yl-acetylamino)-benzyl]-phenyl]-acetamide, termed GN8, efficiently reduced PrP^{Sc}. Subsequently, administration of GN8 was found to prolong the survival of TSE-infected mice. Heteronuclear NMR and computer simulation showed that the specific binding sites are the A-S2 loop (N159) and the region from helix B (V189, T192, and K194) to B-C loop (E196), indicating that the intercalation of these distant regions (hot spots) hampers the pathogenic conversion process. Dynamics-based drug discovery strategy, demonstrated here focusing on the hot spots of PrP^C, will open the way to the development of novel anti-prion drugs.

anti-prion compound | binding sites | chemical chaperone | dynamics-based drug discovery | transmissible spongiform encephalopathy

The accumulation of abnormal protease-resistant prion protein (PrP^{Sc}), a conformational isoform of cellular prion protein (PrP^C), is a key event in the pathogenesis of transmissible spongiform encephalopathies (TSEs) (1–3), and this host-encoded PrP^C has a crucial role in the development of the diseases (4, 5). Because details of the mechanism of conversion from PrP^C to PrP^{Sc} still remain obscure at this stage, PrP^C could be an appropriate molecular target for the drug treatment of TSEs (6) for avoiding the problems associated with the strain differences in PrP^{Sc} (7). PrP^C is a membrane-anchored glycosylated protein and is well conserved in mammals, and its physiological function is currently argued (8). The three-dimensional structure of recombinant PrP^C has been elucidated by NMR (9–13). Briefly, it contains a globular fold with three α-helices (A, B, and C) and a small, imperfectly formed β-sheet (S1 and S2).

The pathogenic conversion process could be related to the thermal stability or the global conformational fluctuation of PrP^C. Recently, a metastable state of the PrP^C was characterized by using a high-pressure NMR (14), where hydrostatic pressure was elevated up to 2,500 bar in an on-line high-pressure NMR cell. The thermodynamical stability profile shows that diverse residues in helices B and C are less stable, indicating the formation of the intermediate conformation (PrP*) (14). Subsequently, a Carr–Purcell–Meiboom–Gill relaxation–dispersion study revealed that slow fluctuation on a time scale of microseconds to milliseconds occurs at the corresponding regions [supporting information (SI) Fig. 4*a*], indicating the conformational rearrangements occurring between the native and the sparsely populated high-energy states (15, 16). Interestingly, mutations related to familial forms of the prion diseases are rather concentrated in helices B and C (SI Fig. 4*b*), and their distribution is somewhat similar to that of slowly fluctuating regions. Moreover, those residues form a major cavity (Fig. 1*a*, green). Thus, a small substance capable of specifically binding to those residues could stabilize the PrP^C conformation because of the decrease in the Gibbs free energy of PrP^C upon binding (6), as well as the suppression of the conformational rearrangements by cross-linking of distant regions. We termed this strategy dynamics-based drug discovery. Because PrP^{Sc} is gradually degraded in *ex vivo* experiments (17, 18), such a population shift toward PrP^C will result in a decrease in PrP^{Sc} population.

Based on dynamics-based drug discovery, we conducted a search for chemical compounds that could specifically bind to the unstable residues. We focused on 14 amino acid residues (M129, G131, N159, V161, Y162, D178, C179, T183, I184, L185, H187, T190, G195, and E196, shown in red with side chain in Fig. 1*a*), located in the loop between helix A and S2 (A-S2 loop) and the loop between helices B and C (B-C loop). A virtual ligand screening program initially picked up 624 chemicals potentially capable of binding to the pocket (Fig. 1*a*, green) with a binding score better (i.e., less) than −32 (SI Table 1), of 320,000 candidates in a database. We further selected the compounds that formed hydrogen bonds with at least one of the 14 amino acids. With careful examination of binding modes, taking into account Lipinski's rules (19), we then selected the 59 compounds showing the lowest predicted binding free energy.

Results

To evaluate the effect of the selected compounds on the conversion of PrP, we next conducted *ex vivo* screening. We used a mouse neuronal cell culture uninfected (GT1-7) and persistently infected with human TSE agent (Fukuoka-1 strain), designated GT+FK (20). Of the 59 compounds, we tested the 44 that were commercially available (see SI Table 1). Among these, 2-pyrrolidin-1-yl-*N*-[4-[4-(2-pyrrolidin-1-yl-acetylamino)-benzyl]-phenyl]-acetamide (compound number 8, molecular weight 420) (Fig. 1*b*) was found to significantly inhibit the PrP^{Sc}

Author contributions: K. Kuwata designed research; K. Kuwata, N.N., T.M., Y.O.K., J.H.-M., K. Kodama, H.K.N., K. Kimura, M.K., Y.T., S.S., J.T., Y.K., and S.K. performed research; H.K.N. analyzed data; K. Kuwata wrote the paper; K. Kuwata performed the NMR measurements and *in silico* screening; N.N. and J.H.-M. performed the *ex vivo* and *in vivo* screening; T.M. prepared the labeled and nonlabeled recombinant PrP; Y.O.K. measured NMR spectra; K. Kodama synthesized GN8; K. Kimura, M.K., Y.T., S.S., and S.K. were mainly engaged in the *in vivo* experiment; and J.T. and Y.K. prepared GN8 aqueous solution for injection and the *in vivo* test.

The authors declare no conflict of interest.

This article is a PNAS Direct Submission.

Abbreviations: TSE, transmissible spongiform encephalopathy; PrP, prion protein; PrP^C, cellular isoform of PrP; PrP^{Sc}, scrapie isoform of PrP; PrP*, sparsely populated high-energy state of PrP; BSE, bovine spongiform encephalopathy; d.p.i., days postinoculation.

[§]To whom correspondence should be addressed. E-mail: kuwata@gifu-u.ac.jp.

This article contains supporting information online at www.pnas.org/cgi/content/full/0702671104/DC1.

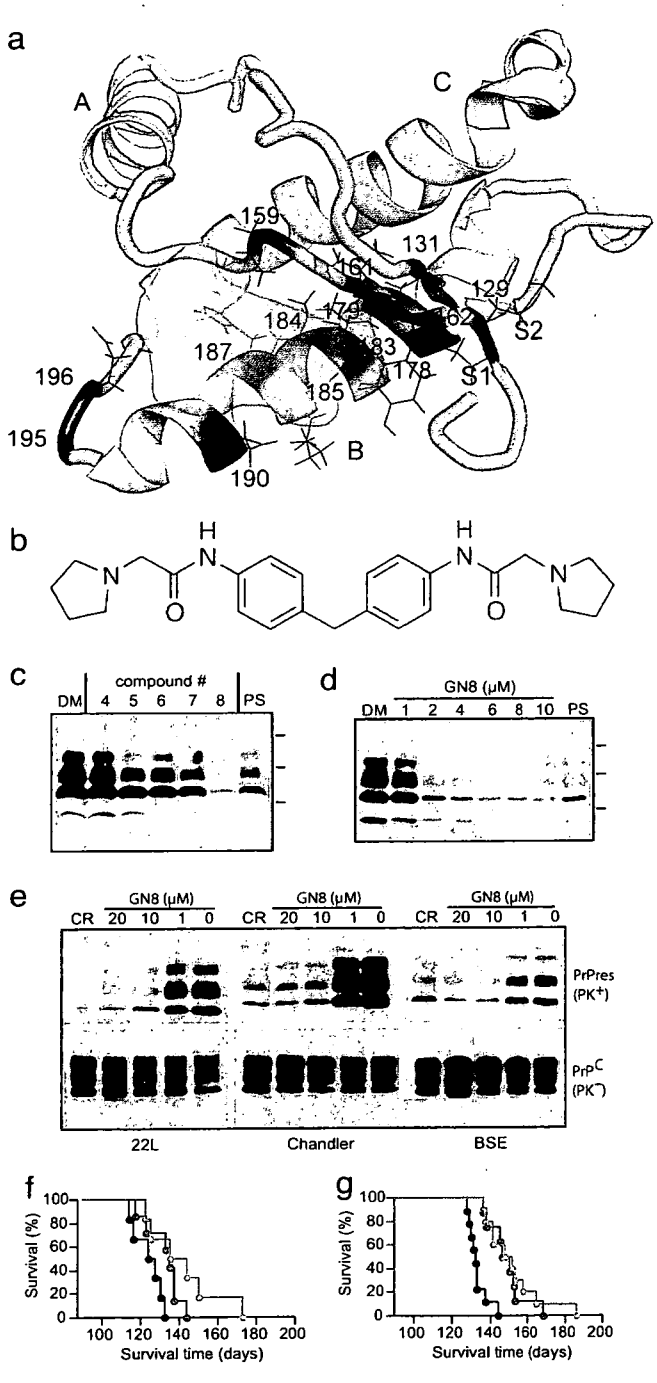

Fig. 1. *In silico* and *ex vivo* screening. (*a*) Residues undergoing global fluctuation displayed as a wire frame in red mapped on the mouse PrP^C structure (residues 124–226) (12), and a binding pocket defined by those residues, colored green. S1, A, S2, B, and C indicate S1 strand, helix A, S2 strand, helix B, and helix C, respectively. The image was created by using PyMol (www.pymol.org). (*b*) 2-Pyrrolidin-1-yl-*N*-[4-[4-(2-pyrrolidin-1-yl-acetylamino)-benzyl]-phenyl]-acetamide, termed GN8. (*c*) Western blotting of PrP^{Sc} in GT+FK cells after treatment with different compounds picked up by *in silico* screening. The cells treated with no. 8 compound showed significant reduction of PrP^{Sc}, which was better than that with 10 μg/ml pentosan polysulfate. DM, DMSO at 0.1%; PS, 10 μg/ml pentosan polysulfate. Molecular masses (37, 25, and 15 kDa) are indicated by bars on the right side of the panels. (*d*) PrP^{Sc} signals in serially diluted mock-treated samples and tested samples were scanned and quantified. The IC_{50} of no. 8 (72-h treatment), as determined by four repeated experiments, was 1.35 μM. (*e*) GN8 reduced PrP^{Sc} also in 22L-, Ch-, and BSE-infected cells. CR, Congo red at 10 μg/ml; PK, proteinase K digestion. (*f*) Kaplan–Meier's survival curves of FK-infected mice administered GN8 by intraventricular infusion. The control group (n = 6) was killed at 123.8 ± 7.4 days (black line). Average survival time of GN8-treated mice was 132.3 ± 9.2 days (42–70 d.p.i. group, n = 7, red line) and 141.5 ± 18.8 days (70–98 d.p.i. group, n = 6, green line). (*g*) Kaplan–Meier's survival curves of FK-infected mice administered GN8 subcutaneously. The control group (n = 9) was killed at 133.0 ± 4.9 days (black line). Average survival time of GN8-treated mice was 148.6 ± 10.3 days (67–95 d.p.i. group, n = 8, red line) and 151.4 ± 15.3 days (67–123 d.p.i. group, n = 10, green line).

production in the GT+FK at 10 μM (Fig. 1*c*). The other compounds either had little effect even at a higher dose (IC_{50} > 100 μM) or were highly toxic to the cells at 1 μM. The effect of the compound (now designated GN8) was dose-dependent (Fig. 1*d*), and by repeating the experiment we established that the effective concentration for 50% reduction of PrP^{Sc} (IC_{50}) over 72 h was ≈1.35 μM. The normal PrP^C expression in uninfected cells was unaffected. A similar effect was confirmed by using other scrapie-infected GT cells (GT+22L and GT+Ch) (20), and also by using GT+BSE cells stably infected with mouse-adapted bovine spongiform encephalopathy (BSE) (Fig. 1*e*). This confirms that the action of GN8 is not strain-specific. To see the effect of GN8 *in vivo*, mice inoculated with 20 μl of 10% FK-1 mouse brain homogenate were given the compound at a dose of 250 μg/kg per day by intraventricular infusion using osmotic pumps (Alzet Durect, Cupertino, CA) during 42–70 days post-inoculation (d.p.i.) or 70–98 d.p.i. Although the vehicle-only control (5% glucose/saline) showed that the average survival time was 123.8 ± 7.4 (n = 6), as expected, the GN8-treated mice showed slightly but significantly prolonged survival even after the appearance of clinical signs [132.3 ± 9.2 days (n = 7) in the 42–70 d.p.i. group and 141.5 ± 18.8 days (n = 6) in the 70–98 d.p.i. group; $P < 0.05$], as shown in Fig. 1*f*. The effect on the survival of infected mice is limited here because of the transient administration of GN8.

The mice administrated subcutaneously with GN8 at a dose of 8.9 mg/kg per day using infusion pumps survived longer than control mice. Whereas the control [5% glucose/saline (63–120 d.p.i. group)] showed that the average survival time was 133.0 ± 4.9 days (n = 9), the GN8-treated mice showed slightly but significantly prolonged survival [148.6 ± 10.3 days (n = 8) in the 67–95 d.p.i. group and 151.4 ± 15.3 days (n = 10) in the 67–123 d.p.i. group; $P < 0.01$], as shown in Fig. 1*g*. Pharmacological analysis using labeled GN8 is currently going on. On the other hand, pentosan polysulfate was not effective at all on the survival time when given peripherally (data not shown). Thus, GN8 could be a potential lead compound for prion diseases.

Binding of GN8 to PrP^C was confirmed by the surface plasmon resonance (21), and its dissociation constant was estimated to be $3.9 \pm 0.2 \times 10^{-6}$ M from the Scatchard plot (Fig. 2*a*; see also SI Fig. 5 and *SI Methods*). To identify the putative sites for interaction of GN8 with PrP, we analyzed the chemical shift perturbation of ^1H-^{15}N heteronuclear single quantum coherence NMR spectra (22) of a uniformly ^{15}N-labeled PrP. A comparison of the spectra revealed that three cross peaks (corresponding to V189, K194, and E196) shifted significantly upon the addition of GN8 (Fig. 2*b*), apparently in a fast-exchange mode. The GN8 concentration did not appear to significantly affect line broadening. Most of the perturbed residues were located in the S2-A loop, the B-helix, or the B-C loop regions, indicating the specific binding between GN8 and PrP^C (Fig. 2*c*). Fig. 2*d* shows the markedly perturbed residues mapped onto a three-dimensional PrP model.

To investigate whether GN8 indeed stabilizes the PrP^C conformation, we measured the thermal stability using CD. The thermal unfolding curves of recombinant mouse PrP, monitored by the molar ellipticity at 222 nm, representing the helical content of PrP and the overall unfolding behavior with (red) or without (blue) GN8, were compared quantitatively (Fig. 2*e* and

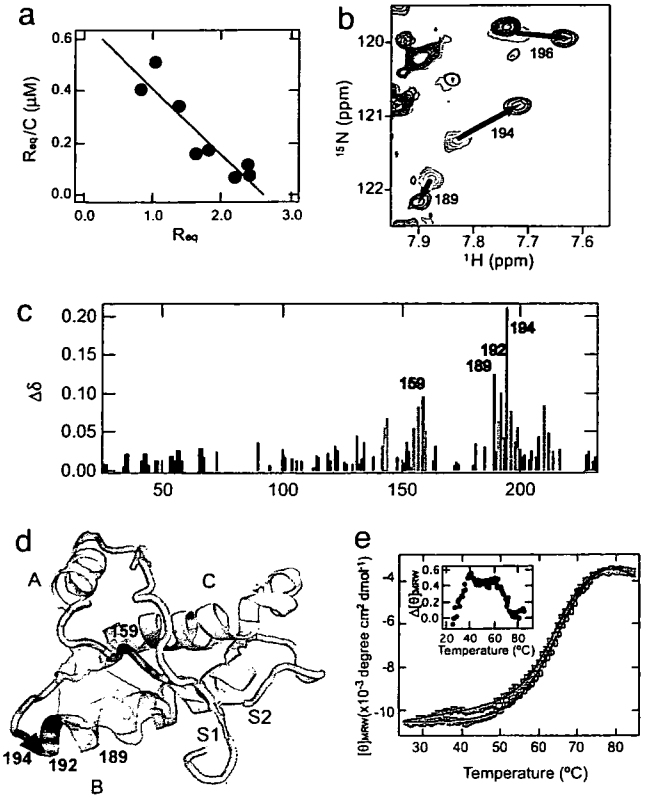

Fig. 2. Interaction of an anti-prion compound, GN8, and a recombinant mouse PrP^C. (*a*) Scatchard plot (Req vs. Req/C, where Req and C are the equilibrium response of SPR and the concentration of GN8, respectively) of the specific binding of GN8 with the PrP obtained by a surface plasmon resonance sensorgram. From the slope of the line, K_d was estimated to be 3.9 μM. (Details are shown in SI Fig. 5 and *SI Methods*.) (*b*) An overlay of the ^1H-^{15}N heteronuclear single quantum coherence NMR spectra of PrP in the absence and presence of GN8. Blue contours show the spectrum of PrP^C without GN8, and red contours show the spectrum in the presence of 1.0 mM GN8 at pH 4.5. (*c*) Plot of the weighted averages of the ^1H and ^{15}N chemical shift changes, calculated by using the function $\Delta\delta = [(\Delta\delta_{1H})^2 + 0.17(\Delta\delta_{15N})^2]^{1/2}$ against the residue number. The absence of bars in the plot indicates unassigned residues, proline residues, or unmeasured shifts due to resonance overlaps. Perturbed residues with $\Delta\delta$ values of >0.9 ppm are shown in red, and those with 0.9 > $\Delta\delta$ > 0.5 ppm are in orange. (*d*) Mapping of the perturbed residues on the structure of mPrP(121–231) (PDB entry 1AG2). The perturbed residues with $\Delta\delta$ values of >0.9 ppm are shown in red, and those with 0.9 > $\Delta\delta$ > 0.5 ppm are in orange. Binding pocket is overlaid in green. S1, A, S2, B, and C indicate S1 strand, helix A, S2 strand, helix B, and helix C, respectively. The image was created by using PyMol. (*e*) Thermal unfolding profiles of recombinant mouse PrP (amino acids 23–231, 5 μM) without (blue) or with (red) GN8 (10 μM). CD intensities of PrP in the presence of GN8 were normalized to those of PrP without GN8, and fitted curves (see *SI Methods*) are also shown. Binding with GN8 stabilizes the conformation of PrP^C. (*Inset*) The difference in extinction coefficients at 222 nm of PrP without GN8 and those in the presence of GN8, as a function of temperature.

SI Methods). Parameter sets obtained by a nonlinear fit, i.e., melting temperature (T_m) and enthalpy change (ΔH), without GN8 were 65.3 ± 0.4°C and 35.0 ± 1.9 kcal/mol, respectively, whereas those with GN8 were 67.7 ± 0.6°C and 41.8 ± 2.2 kcal/mol, respectively. This indicates that the binding of GN8 stabilizes the PrP^C conformation significantly. Intriguingly, the accumulation of the intermediate was demonstrated by an early increase in ellipticity at ≈40°C before the global unfolding as shown in Fig. 2*e Inset*. However, this is strongly suppressed in the presence of GN8. Thus, GN8 suppressed the production of both PrP^{Sc} (Fig. 1 *c–e*) and PrP^U (thermally unfolded state) (Fig. 2*e*) by reducing the intermediate population (14).

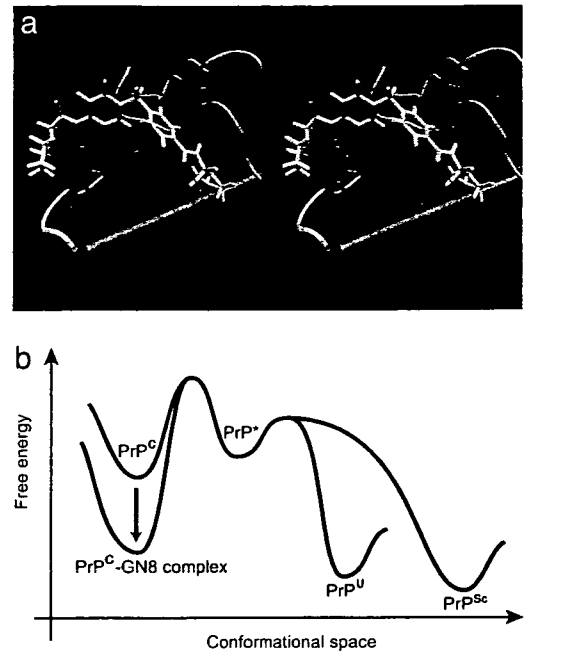

Fig. 3. Inhibitory mechanism of GN8 for pathogenic conversion. (*a*) Stereoview of the optimized complex structure of the GN8 and mouse PrP^C, with putative hydrogen bonds, calculated by using ICM version 3.0. Presumed hydrogen bonds between GN8 (green) and E196 (red) and between GN8 (green) and N159 (blue) are shown in orange (dotted lines). The images were created with VMD (52). (*b*) Illustration of the Gibbs free energy as a function of the conformational space to explain the inhibitory mechanism of a chemical chaperone, GN8. GN8 stabilizes the PrP^C conformation and reduces the population of PrP*, PrP^{Sc}, and PrP^U. PrP* may not interact with GN8, because the specific conformation around the binding sites would be lost (14). Thus, the free energy level of PrP*, PrP^U, and PrP^{Sc} would not change much in the presence of GN8.

Discussion

The structure of the PrP^C–GN8 complex was further analyzed by computer simulation using the refined energy minimization procedure with flexible receptor side chain. GN8 (Fig. 3*a*) connected distant residues, N159 (A-S2 loop) and E196 (B-C loop), by hydrogen bonds. The regions with the significant chemical shift changes described above (Fig. 2*d*) were in good agreement with the binding regions of GN8 in the simulated structure of the prion–GN8 complex (Fig. 3*a*). Intriguingly, K194 at the C terminus of the helix B and E196 in the B-C loop undergo slow exchange dynamics (16) (SI Fig. 4*b*). Indeed, the mutation E196K causes a rapidly progressive dementia and ataxia (23) and could be expected to greatly reduce the protein stability because of the elimination of salt bridges between E196, R156, and K194 (23).

Intercalation of these two binding regions (A-S2 loop and B-C loop) may be essential to stabilize the PrP^C conformation. For example, two representative binding sites, N159 and E196, are close together (distance between C_α atoms ≈ 15.4 Å) in PrP^C structure (12), but in the hypothetical PrP^{Sc} structure (24) they are considerably more distant (distance between C_α atoms ≈ 45.2 Å). Because GN8 connects distant regions (N159 and E196) in the PrP sequence (36 aa) by hydrogen bonds, large conformational shift may be significantly prohibited, and thus intermediate (PrP*) and further PrP^{Sc} or PrP^U formation may be also blocked.

Matsuda *et al.* (25) reported about the chemical chaperone therapy for GM1-gangliosidosis, but there has been no direct evidence for such a mechanism working on the anti-prion com-

pounds. Experimental evidences presented here fully support the concept that GN8 acts as a chemical chaperone to stabilize the normal prion protein (PrP) conformation. As illustrated in Fig. 3*b*, free energy of PrP^C–GN8 complex is significantly less than that of PrP^C, so the populations of the transition state, PrP^*, PrP^U, and PrP^{Sc} may be reduced accordingly.

Over the past 10 years there have been various efforts to find out small compounds to reduce PrP^{Sc} population. These include porphyrins (26, 27), Congo red and its derivatives (28–30), acridine and phenothiazine derivatives (17, 31, 32), heparan sulfate (33), aminoglycan, and polyamines (34, 35). Simultaneously, various technological developments have been reported including structure-based drug design (36) followed by the structure–activity relationship study (37), small interfering RNA (38), library screening (18), high-throughput screening (39), chimeric ligand approach (40), and so on. Although strategies for drug discovery used in these studies have a broad spectrum from empirical to rational preponderance, there has been no report on the residue-specific evidences for the binding regions of anti-prion compounds. For instance, the effect of BF-168 depends on the strains (41), suggesting that BF-168 may not interact with PrP^C but with PrP^{Sc} in a strain-dependent manner, but this is still indirect evidence.

The structure of GN8 somewhat resembles a number of other small PrP^{Sc} inhibitors, such as the Congo red, which is able to interact with the N-terminal domain of PrP^C (42). However, we could not find out any evidence for the interaction between GN8 and the N-terminal domain. The inhibitory mechanism of GN8 and that of Congo red seem to be quite different because of the following reasons: (*i*) Congo red has two sulfonates on the edge of the molecule, but GN8 does not have negative charge. Thus, GN8 may not strongly interact with His+ at the octapeptide repeats of the N-terminal domain. (*ii*) Although Congo red can cause aggregation of recombinant PrP^C (42), GN8 never causes aggregation even at a relatively high concentration (≈0.03 mM) in NMR tube. (*iii*) Chemical shift changes caused by binding with GN8 are not significant at the N-terminal half region as shown in Fig. 2*c*. (*iv*) SPR affinity profile between GN8 and the C-terminal half of PrP^C(120–230) and that between GN8 and the full-length PrP^C(23–231) were quite similar, and the calculated dissociation constants were also close (≈5 μM), supporting our conclusion that the major binding regions of GN8 locate at the C-terminal domain. On the other hand, the interaction sites of GN8 with the GPI-anchored PrP^C on the cell surface could be different from those with the free PrP^C. However, a carboxymethyl moiety on the SPR sensor chip has a negative charge like a phosphate moiety on the cell membrane. Because electrostatic environments surrounding GN8 and prion on these surfaces are similar, GN8 may also interact with the C-terminal domain of the GPI-anchored PrP^C.

We found here the effective anti-prion compound GN8, which specifically binds with the hot spots undergoing the slow fluctuation on the time scale of microseconds to milliseconds and exclusively interferes with the pathogenic conversion. According to the dynamics-based drug discovery strategy, we found >20 compounds with any anti-prion activity, and the hit rate is ≈10% at present (data not shown). However, no compound has been more effective than GN8. For instance, we found a compound, GN4 (see SI Table 1), whose structure is quite similar to GN8, but the computer simulation suggested that the binding sites are R156 and N159, which are quite close (2 aa). Thus, GN4 is expected to have less inhibitory effect on the global fluctuation of PrP^C, and indeed IC_{50} of GN4 was >100 μM (data not shown).

To potentially become of any use clinically, GN8 will need to clear many pharmacological hurdles; however, our basic principle presented here constitutes a promising strategy with which to approach the discovery of therapeutic compounds for TSE. Additionally, application of the dynamics-based drug discovery approach, based on the experimentally identified hot spot (43), will make the mass screening of chemical compounds more efficient, especially for diseases related to protein misfolding (44).

Materials and Methods

Virtual Ligand Screening. We performed *in silico* screening of ligands on 320,000 compounds in the Available Chemicals Directory (MDL Information Systems, San Leandro, CA) for specific binding to mouse PrP^C (12). Residues with the exchange time constant, τ_{ex}, between two sites of >10 ms are displayed in SI Fig. 4*a* (16). The software used was ICM version 3.0 (Molsoft, La Jolla, CA). The program, by global optimization of the entire flexible ligand in the receptor (mouse PrP^C) field (45), came up with 624 candidates potentially capable of binding to the pocket with a binding score better (i.e., less) than −32, which roughly corresponds to binding energy (kcal/mol). Then, a more refined energy-minimization procedure using a flexible receptor side chain was conducted and further selected the compounds that formed hydrogen bonds with at least one of the 14 amino acids.

Chemical Compounds. Chemical compounds selected from our virtual ligand screening simulation were purchased from Aldrich Chemical Company (Milwaukee, WI), G & J Research Chemicals (Devon, U.K.), Wako Pure Chemical (Osaka, Japan), Interchim (Montlucon, France), Labotest (Niederschoena, Germany), Florida Center for Heterocyclic Compounds (Gainesville, FL), ChemBridge (San Diego, CA), Maybridge Chemical Company (Cornwall, U.K.), TimTec (Newark, NJ), Ambinter (Paris, France), Oak Samples (Kier, U.K.), Scientific Exchange (Center Ossipee, NH), ChemStar (Moscow, Russia), ChemDiv (San Diego, CA), and AsInEx (Moscow, Russia), or kindly provided by the Drug Synthesis and Chemistry Branch, Developmental Therapeutic Program, Division of Cancer Treatments and Diagnosis, National Cancer Institute. Detailed information on the sources for all of the compounds is shown in SI Table 1. The compounds were dissolved with DMSO for the *in vitro* screening and with distilled water for the spectral measurements. GN8 hydrochloride salt was prepared for *in vivo* test as follows: GN8 was first dissolved with dioxane and added to 3 N HCl in dioxane. The solvent was evaporated *in vacuo*, and the residue was recrystallized from acetone to give the hydrochloride salt of GN8. GN8 hydrochloride salt (2-pyrrolidin-1-yl-*N*-[4-[4-(2-pyrrolidin-1-yl-acetylamino)-benzyl]-phenyl]-acetamide dihydrochloride); white solid; anal. calcd. for $C_{25}H_{34}Cl_2N_4O_2$: C, 60.85; H, 6.94; Cl, 14.37; N, 11.35; O, 6.48. %Found: C, 60.83; H, 6.95; N, 11.35.

Recombinant Mouse PrP. The DNA of mouse PrP(23–231) was amplified by PCR and cloned into the expression vector pET101/D-TOPO (Invitrogen, Carlsbad, CA). As shown in *SI Methods*, the ^{15}N-labeled recombinant PrP for NMR measurements was expressed in *Escherichia coli* strain BL21 Star (DE3) (Invitrogen), grown in ^{15}N-labeled minimum medium Spectra9 (Spectra Gases, Branchburg, NJ), and purified by a Ni-chelating affinity chromatography method (46). Oxidization and refolding of the purified protein (47) were performed in buffer containing 4 M urea at pH 8. A recombinant PrP sample for the surface plasmon resonance sensorgram experiment was obtained by a similar procedure using a non-isotope-labeled LB medium instead of the Spectra9.

Cell Culture and Antibodies. The immortalized mouse neuronal cell line GT1-7 was cultured as described (20). GT1-7 cells stably infected with Fukuoka-1, 22L, or Chandler/RML (designated GT+FK, GT+22L, or GT+Ch, respectively) were maintained for more than a year in our laboratory. GT+BSE cells were infected *ex vivo* in our laboratory with mouse-adapted BSE agent (a kind gift from T. Yokoyama, National Institute of Animal Health, Tsukuba, Japan). Stock solutions of compounds were prepared fresh in 100%

DMSO at 100 mM and stored at 4°C. Before use, compounds were diluted with medium as indicated. Control cells were treated with medium containing solvent alone (0.1%). Approximately 2×10^5 cells were plated in each well of a six-well plate, and drug treatment was started 15 h later. After 72 h of incubation, cells were lysed in 150 μl of 1× Triton X-100/DOC lysis buffer (48), and samples normalized to 2 mg of protein per milliliter. Western blotting for PrP^{Sc} was done as described previously (48). Anti-mouse PrP antisera (SS28) (49) and SAF32 antibody (SPI-BIO, Montigny le Bretonneux, France) were used for PrP^{Sc} and PrP^{C}, respectively, as the primary antibody. The signals were visualized by ECL-plus (Amersham, Buckinghamshire, U.K.) and scanned by using FluorChem (Alpha Innotech, San Leandro, CA).

NMR Measurements and Data Analysis. For NMR measurements, 0.6 mg/ml ^{15}N-uniformly labeled mouse PrP(23–231) was prepared in 30 mM acetate-d_3 buffer (pH 4.5) containing 1 mM NaN_3, 4.5 μM 4-(2-aminoethyl)-benzenesulfonyl fluoride hydrochloride, 20 μM EDTA, 0.4 μM Bestatin, 0.06 μM pepstatin, 0.06 μM E-64, and 1 nM sodium 2,2-dimethyl-2-silapentane-5-sulfonate dissolved in 90% H_2O/10% D_2O. NMR spectra were recorded at 20.0°C on an Avance600 spectrometer (Bruker, Rheinstetten, Germany) at Gifu University. The spectrometer operates at ^1H frequency of 600.13 MHz and ^{15}N frequency of 60.81 MHz. A 5-mm ^1H inverse detection probe with triple-axis gradient coils was used for all measurements. ^1H-^{15}N heteronuclear single quantum coherence spectra were acquired with 2,048 complex points covering 9,600 Hz for ^1H and 256 complex points covering 1,200 Hz for ^{15}N. NMR data were processed by using the XWIN-NMR software package (Bruker) and Sparky (50). Resonance frequencies in these spectra were identified by using the chemical shift lists on mouse PrP(23–231) and PrP (121–231) (51). For the chemical shift perturbation experiments, aliquots of 2.5 μl of 0, 10, or 100 mM GN8 solutions in DMSO-d_6 were added to 0.6 mg/ml ^{15}N PrP(23–231) in a 5-mm-diameter Shigemi microtube; the final concentration of GN8 is 0, 1, and 10 mM, respectively. The backbone ^1H and ^{15}N chemical shifts for the GN8-bound protein were assigned by tracing the corresponding peaks in ^1H-^{15}N heteronuclear single quantum coherence spectra measured at various concentrations of GN8.

Preparation of GN8 for Injection and *in Vivo* Test. The GN8 hydrochloride salt was dissolved in saline with 5% glucose and sterilized by passing through a 0.2-μm filter. The concentration of the stock solution was adjusted to 10 mg/ml and kept at 4°C until use. Ten percent FK-infected brain homogenate was inoculated into right temporal lobes of 4-week-old male mice (ddY), followed by intraventricular infusion of GN8 using an osmotic pump. Six or 10 weeks after inoculation, an osmotic pump was inserted subcutaneously and the infusion cannula was implanted into the right ventricle. The pump was filled with GN8 (1.4 mg/ml) or saline with 5% glucose. In a parallel experiment, pentosan polysulfate (Bene, Munich, Germany) was administered at 200 μg/kg per day by intraventricular or i.p. infusion. All mice were carefully examined daily for neurological signs, and the incubation period was monitored. Survival data were statistically evaluated according to Kaplan–Meier's method using StatMateIII (ATMS, Tokyo, Japan).

In case of subcutaneous infusion of GN8, the concentration of the stock solution was adjusted to 50 mg/ml. One percent FK-infected brain homogenate was inoculated in the same way, and an osmotic pump including GN8 was inserted subcutaneously at 9 weeks after inoculation.

Some compounds were kindly provided by the Drug Synthesis and Chemistry Branch, Developmental Therapeutic Program, Division of Cancer Treatments and Diagnosis, National Cancer Institute. We thank Ms. Sakiko Morishita and Mr. Yuki Matsui for technical help. K. Kuwata was supported in part by Grants-in-Aid for Scientific Research from the Ministry of Education, Culture, Sports, Science and Technology of Japan and grants from the Ministry of Health, Labour, and Welfare. This study was supported by the Program for Promotion of Fundamental Studies in Health Sciences of the National Institute of Biomedical Innovation.

1. Prusiner SB (1982) *Science* 216:136–144.
2. Prusiner SB (1991) *Crit Rev Biochem Mol Biol* 26:397–438.
3. Prusiner SB (1998) *Proc Natl Acad Sci USA* 95:13363–13383.
4. Bueler H, Aguzzi A, Sailer A, Greiner RA, Autenried P, Aguet M, Weissmann C (1993) *Cell* 73:1339–1347.
5. Sailer A, Bueler H, Fischer M, Aguzzi A, Weissmann C (1994) *Cell* 77:967–968.
6. Cohen FE, Pan KM, Huang Z, Baldwin M, Fletterick RJ, Prusiner SB (1994) *Science* 264:530–531.
7. Peretz D, Williamson RA, Legname G, Matsunaga Y, Vergara J, Burton DR, DeArmond SJ, Prusiner SB, Scott MR (2002) *Neuron* 34:921–932.
8. Zhang CC, Steele AD, Lindquist S, Lodish HF (2006) *Proc Natl Acad Sci USA* 103:2184–2189.
9. Donne DG, Viles JH, Groth D, Mehlhorn I, James TL, Cohen FE, Prusiner SB, Wright PE, Dyson HJ (1997) *Proc Natl Acad Sci USA* 94:13452–13457.
10. James TL, Liu H, Ulyanov NB, Farr-Jones S, Zhang H, Donne DG, Kaneko K, Groth D, Mehlhorn I, Prusiner SB, Cohen FE (1997) *Proc Natl Acad Sci USA* 94:10086–10091.
11. Gossert AD, Bonjour S, Lysek DA, Fiorito F, Wuthrich K (2005) *Proc Natl Acad Sci USA* 102:646–650.
12. Riek R, Hornemann S, Wider G, Billeter M, Glockshuber R, Wuthrich K (1996) *Nature* 382:180–182.
13. Lysek DA, Schorn C, Nivon LG, Esteve-Moya V, Christen B, Calzolai L, von Schroetter C, Fiorito F, Herrmann T, Guntert P, Wuthrich K (2005) *Proc Natl Acad Sci USA* 102:640–645.
14. Kuwata K, Li H, Yamada H, Legname G, Prusiner SB, Akasaka K, James TL (2002) *Biochemistry* 41:12277–12283.
15. Korzhnev DM, Salvatella X, Vendruscolo M, Di Nardo AA, Davidson AR, Dobson CM, Kay LE (2004) *Nature* 430:586–590.
16. Kuwata K, Kamatari YO, Akasaka K, James TL (2004) *Biochemistry* 43:4439–4446.
17. Doh-Ura K, Iwaki T, Caughey B (2000) *J Virol* 74:4894–4897.
18. Kocisko DA, Baron GS, Rubenstein R, Chen J, Kuizon S, Caughey B (2003) *J Virol* 77:10288–10294.
19. Lipinski CA, Lombardo F, Dominy BW, Feeney PJ (2001) *Adv Drug Deliv Rev* 46:3–26.
20. Milhavet O, McMahon HE, Rachidi W, Nishida N, Katamine S, Mange A, Arlotto M, Casanova D, Riondel J, Favier A, Lehmann S (2000) *Proc Natl Acad Sci USA* 97:13937–13942.
21. Touil F, Pratt S, Mutter R, Chen B (2006) *J Pharm Biomed Anal* 40:822–832.
22. Zuiderweg ER (2002) *Biochemistry* 41:1–7.
23. Peoc'h K, Manivet P, Beaudry P, Attane F, Besson G, Hannequin D, Delasnerie-Laupretre N, Laplanche JL (2000) *Hum Mutat* 15:482.
24. Govaerts C, Wille H, Prusiner SB, Cohen FE (2004) *Proc Natl Acad Sci USA* 101:8342–8347.
25. Matsuda J, Suzuki O, Oshima A, Yamamoto Y, Noguchi A, Takimoto K, Itoh M, Matsuzaki Y, Yasuda Y, Ogawa S, *et al.* (2003) *Proc Natl Acad Sci USA* 100:15912–15917.
26. Caughey WS, Raymond LD, Horiuchi M, Caughey B (1998) *Proc Natl Acad Sci USA* 95:12117–12122.
27. Priola SA, Raines A, Caughey WS (2000) *Science* 287:1503–1506.
28. Caspi S, Halimi M, Yanai A, Sasson SB, Taraboulos A, Gabizon R (1998) *J Biol Chem* 273:3484–3489.
29. Milhavet O, Mange A, Casanova D, Lehmann S (2000) *J Neurochem* 74:222–230.
30. Sellarajah S, Lekishvili T, Bowring C, Thompsett AR, Rudyk H, Birkett CR, Brown DR, Gilbert IH (2004) *J Med Chem* 47:5515–5534.
31. Korth C, May BC, Cohen FE, Prusiner SB (2001) *Proc Natl Acad Sci USA* 98:9836–9841.
32. May BC, Fafarman AT, Hong SB, Rogers M, Deady LW, Prusiner SB, Cohen FE (2003) *Proc Natl Acad Sci USA* 100:3416–3421.
33. Adjou KT, Simoneau S, Sales N, Lamoury F, Dormont D, Papy-Garcia D, Barritault D, Deslys JP, Lasmezas CI (2003) *J Gen Virol* 84:2595–2603.
34. Perez M, Wandosell F, Colaco C, Avila J (1998) *Biochem J* 335:369–374.
35. Supattapone S, Nguyen HO, Cohen FE, Prusiner SB, Scott MR (1999) *Proc Natl Acad Sci USA* 96:14529–14534.
36. Perrier V, Wallace AC, Kaneko K, Safar J, Prusiner SB, Cohen FE (2000) *Proc Natl Acad Sci USA* 97:6073–6078.
37. May BC, Zorn JA, Witkop J, Sherrill J, Wallace AC, Legname G, Prusiner SB, Cohen FE (2007) *J Med Chem* 50:65–73.
38. Daude N, Marella M, Chabry J (2003) *J Cell Sci* 116:2775–2779.

39. Bertsch U, Winklhofer KF, Hirschberger T, Bieschke J, Weber P, Hartl FU, Tavan P, Tatzelt J, Kretzschmar HA, Giese A (2005) *J Virol* 79: 7785–7791.
40. Dollinger S, Lober S, Klingenstein R, Korth C, Gmeiner P (2006) *J Med Chem* 49:6591–6595.
41. Ishikawa K, Kudo Y, Nishida N, Suemoto T, Sawada T, Iwaki T, Doh-ura K (2006) *J Neurochem* 99:198–205.
42. Caughey B, Caughey WS, Kocisko DA, Lee KS, Silveira JR, Morrey JD (2006) *Acc Chem Res* 39:646–653.
43. Clackson T, Wells JA (1995) *Science* 267:383–386.
44. Soto C, Estrada L, Castilla J (2006) *Trends Biochem Sci* 31:150–155.
45. Schapira M, Raaka BM, Samuels HH, Abagyan R (2000) *Proc Natl Acad Sci USA* 97:1008–1013.
46. Bocharova OV, Breydo L, Parfenov AS, Salnikov VV, Baskakov IV (2005) *J Mol Biol* 346:645–659.
47. Lu BY, Beck PJ, Chang JY (2001) *Eur J Biochem* 268:3767–3773.
48. Nishida N, Harris DA, Vilette D, Laude H, Frobert Y, Grassi J, Casanova D, Milhavet O, Lehmann S (2000) *J Virol* 74:320–325.
49. Nishida N, Tremblay P, Sugimoto T, Shigematsu K, Shirabe S, Petromilli C, Erpel SP, Nakaoke R, Atarashi R, Houtani T, *et al.* (1999) *Lab Invest* 79:689–697.
50. Goddard TD, Kneller DG (2001) SPARKY (Univ of California, San Francisco), Version 3.
51. Riek R (1988) PhD thesis (Swiss Federal Institute of Technology, Zürich, Switzerland).
52. Humphrey W, Dalke A, Schulten K (1996) *J Mol Graphics* 14:27–28, 33–38.

J Neurol (2007) 254:1509–1517
DOI 10.1007/s00415-007-0540-9

ORIGINAL COMMUNICATION

Yusei Shiga
Katsuya Satoh
Tetsuyuki Kitamoto
Sigenori Kanno
Ichiro Nakashima
Shigeru Sato
Kazuo Fujihara
Hiroshi Takata
Keigo Nobukuni
Shigetoshi Kuroda
Hiroki Takano
Yoshitaka Umeda
Hidehiko Konno
Kunihiko Nagasato
Akira Satoh
Yoshito Matsuda
Mitsuru Hidaka
Hirokatsu Takahashi
Yasuteru Sano
Kang Kim
Takashi Konishi
Katsumi Doh-ura
Takeshi Sato
Kensuke Sasaki
Yoshikazu Nakamura
Masahito Yamada
Hidehiro Mizusawa
Yasuto Itoyama

Two different clinical phenotypes of Creutzfeldt-Jakob disease with a M232R substitution

Received: 28 June 2006
Received in revised form: 8 January 2007
Accepted: 6 February 2007
Published online: 2 November 2007

Y. Shiga, MD, PhD* (✉) · S. Kanno, MD · I. Nakashima, MD, PhD · K. Fujihara, MD, PhD · Y. Itoyama, MD, PhD
Dept. of Neurology
Tohoku University Graduate School of Medicine
1-1 Seiryo-machi, Aoba-ku
Sendai 980-8574, Japan
Tel.: +81-22/717-7189
Fax: +81-22/717-7192
E-Mail:
yshiga@em.neurol.med.tohoku.ac.jp

K. Satoh, MD, PhD
The First Department of Internal Medicine
Graduate School of Medicine
Nagasaki University, Japan

T. Kitamoto, MD, PhD*
Division of CJD Science and Technology
Graduate School of Medicine
Tohoku University, Japan

S. Sato, MD, PhD
Dept. of Neurology
Kohnan Hospital, Japan

H. Takata, MD, PhD · K. Nobukuni, MD, PhD
Dept. of Neurology
Minami Okayama National Hospital, Japan

S. Kuroda, MD, PhD*
Dept. of Neuropsychiatry
Graduate School of Medicine, Dentistry and Pharmaceutical Sciences
Okayama University, Japan

H. Takano, MD, PhD · Y. Umeda, MD, PhD
Dept. of Neurology
Brain Research Institute
Niigata University, Japan

H. Konno, MD, PhD
Dept. of Neurology
Nishitaga National Hospital, Japan

K. Nagasato, MD, PhD
Dept. of Neurology
Isahaya General Hospital, Japan

A. Satoh, MD, PhD
Dept. of Neurology
Nagasaki Kita Hospital, Japan

Y. Matsuda, MD, PhD
Dept. of Neuropsychiatry
Graduate School of Medicine
Yamaguchi University, Japan

M. Hidaka, MD, PhD
Yokohama Miyazaki Hospital of Neurosurgery, Japan

H. Takahashi, MD, PhD
Dept. of Neurology
Matsudo Municipal Hospital, Japan

Y. Sano, MD, PhD
Dept. of Neurology
Graduate School of Medicine
Yamaguchi University, Japan

K. Kim, MD, PhD
Dept. of Neurology
Shizuoka General Hospital, Japan

T. Konishi, MD, PhD
Dept. of Neurology
Shizuoka National Medical Center, Japan

K. Doh-ura, MD, PhD
Division of Prion Protein Biology
Graduate School of Medicine
Tohoku University, Japan

T. Sato, MD, PhD*
National Center for Neurology and Psychiatry
Kohnodai Hospital, Japan

K. Sasaki, MD, PhD
Dept. of Neuropathology
Neurological Institute
Graduate School of Medical Sciences
Kyushu University, Japan

Y. Nakamura, MD, PhD*
Dept. of Public Health
Jichi Medical School, Japan

M. Yamada, MD, PhD*
Depts. of Neurology and Neurobiology of Aging
Graduate School of Medical Science
Kanazawa University, Japan

H. Mizusawa, MD, PhD*
Dept. of Neurology and Neurological Science
Graduate School
Tokyo Medical and Dental University, Japan

* The Creutzfeldt-Jakob Disease Surveillance Committee, Japan.

JON 2540

Abstract *Objective* To describe the clinical features of Creutzfeldt-Jakob disease with a substitution of arginine for methionine (M232R substitution) at codon 232 (CJD232) of the prion protein gene (PRNP). *Patients and methods* We evaluated the clinical and laboratory features of 20 CJD232 patients: age of onset, initial symptoms, duration until becoming akinetic and mute, duration until occurrence of periodic sharp and wave complexes on EEG (PSWC), MRI findings, and the presence of CSF 14-3-3 protein. Immunohistochemically, prion protein (PrP) deposition was studied. *Results* None of the patients had a family history of CJD. We recognized two clinical phenotypes: a rapidly progressive type (rapid-type) and a slowly progressive type (slow-type). Out of 20 patients, 15 became akinetic and mute, demonstrated myoclonus, and showed PSWC within a mean duration of 3.1, 2.4, and 2.8 months, respectively (rapid-type). Five showed slowly progressive clinical courses (slow-type). Five became akinetic and mute and four demonstrated myoclonus within a mean duration of 20.6 and 15.3 months, respectively, which were significantly longer than those in the rapid-type. Only one demonstrated PSWC 13 months after the onset. Diffuse synaptic-type deposition was demonstrated in four rapid-type patients, and perivacuolar and diffuse synaptic-type deposition in two, and diffuse synaptic-type deposition in one slow-type patient. Three of 50 suspected but non-CJD patients had the M232R substitution. *Conclusions* Patients with CJD232 had no family history like patients with sCJD, and showed two different clinical phenotypes in spite of having the same PRNP genotype. More studies are needed to determine whether M232R substitution causes the disease and influences the disease progression.

Key words Creutzfeldt-Jakob disease · M232R · clinical phenotype · uncommon variant · diffusion-weighted MRI

Introduction

Human prion diseases are divided into three types: sporadic, genetic, and infectious prion disease. Genetic prion disease, which is defined as prion disease with causative abnormalities of the prion protein gene (PRNP), accounts for approximately 10 to 15% of all prion disease cases, and includes genetic Creutzfeldt-Jakob disease (gCJD), Gerstmann-Sträussler-Scheinker disease (GSS), and fatal familial insomnia (FFI) [1]. In general, the clinical features of gCJD are more various compared with those of sporadic CJD (sCJD) and are regulated by the genotype [2]. Therefore, gCJD, even if its clinical features are quite different from those of sCJD, especially those of the most often encountered type of sCJD with methionine homozygosity at codon 129 of PRNP and type 1 protease-resistant prion protein (MM1) [3], can be diagnosed by examining the genotype. To clarify the clinical features of CJD, which associates with a substitution in PRNP, will provide an important clue that can lead to genetic examination.

To date, more than 30 causative mutations have been recognized and individual PRNP mutations show variable geographical distribution and frequency. The cardinal characteristic of gCJD is that more than half of the patients lack family history.

CJD patients associated with a substitution of arginine for methionine at codon 232 (M232R substitution) in PRNP with no relevant family history have been reported in Japan [4–10]. Previously, the clinical features of CJD with the M232R substitution (CJD232) were thought to be similar to those of typical sCJD with MM1 [3], which accounts for the vast majority of sCJD in terms of clinical features, including EEG findings [5, 6, 9]. However, cases of CJD232 that showed a longer clinical course and lacked the characteristic periodic sharp and wave complexes (PSWC) have been reported [7, 8]. We have experienced eight cases of CJD232. Five of them showed a rapid clinical course and typical CJD features, while the others showed very slow progression and atypical features. We studied the clinical features of 20 CJD232 patients, including our original patients, and found that there were two different major clinical phenotypes with the same genotype, including polymorphisms at codons 129 and 219 of PRNP; one progressed rapidly, and the other progressed slowly. Better understanding of the clinical features of CJD232 would contribute to the diagnosis of CJD232, especially in patients with atypical clinical features.

Patients and methods

Twenty-four patients with CJD232 were included in this study: eight were our original cases, seven were obtained by reviewing the literature [5–10] and nine were found by reviewing the clinical records of CJD patients reported to the Creutzfeldt-Jakob disease Surveillance Committee, Japan. We excluded two patients because they had double point mutations at codon 180 and at codon 232 [10] and one patient because her polymorphism at codons 129 and 219 of PRNP was uncertain [5]. Therefore, 21 patients were enrolled in this study. The nine who were proven at autopsy are indicated by asterisks in Fig. 1.

We first evaluated the duration from onset until the patients manifested akinetic mutism. As shown in Fig. 1, 15 became akinetic and mute within six months, while five did not become so until 15 months after the onset. These CJD232 patients appeared to be comprised of two different groups: one was a rapidly progressive type (rapid-type) and the other was a slowly progressive type (slow-type). We evaluated the age of onset, initial symptoms, duration from onset to the appearance of myoclonus, duration from onset to akinetic mutism, du-

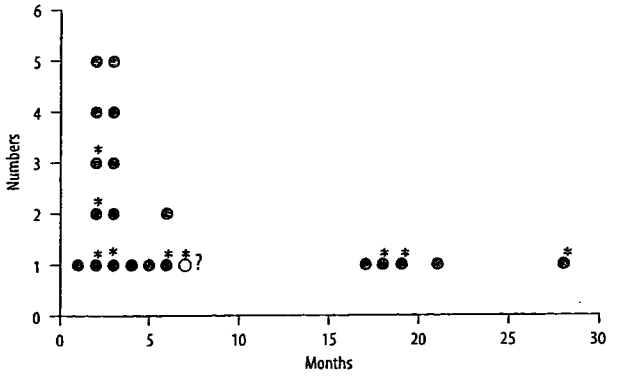

Fig. 1 The duration from the onset to akinetic mutism. The X-axis shows the duration (months) and the Y-axis shows the accumulative number of patients. Black circles indicate patients who became akinetic and mute; the white circle indicates a patient who had not become akinetic and mute. The white circle with a question mark indicates a 50-year-old-male patient who suddenly died seven months after the onset because of a myocardial incident. Since he had not become akinetic and mute, and was able to converse with simple words, we excluded him from further analyses. Asterisks indicate autopsy proven patients. We recognize two different groups concerning the duration from the onset to akinetic mutism: a rapidly progressive type and a slowly progressive type

ration from onset to occurrence of PSWC, results of MRI, and the presence of 14-3-3 protein in the CSF of the two types. The patient marked by a question mark in Fig. 1 was excluded from the evaluation. We were unable to determine which group this 50-year-old man belonged to because he had not become akinetic and mute and was still able to converse with simple words seven months after the onset when he suddenly died due to a myocardial incident [8]. Thus, the clinical data of 20 patients were finally used for this study.

In one of the rapid-type patients and in three of the slow-type patients including a previously reported 64-year-old woman [7], immunohistochemical staining of PrP using monoclonal antibody 3F4 (Prionics, Schlieren, Switzerland) was performed. Including the previously reported pathological findings of three patients belonging to the rapid-type [6], immunohistochemical staining of PrP in both groups were studied. In each group, the molecular type of the abnormal isoform of prion protein (PrP^{Sc}) was studied.

The Mann-Whitney U test was used for statistical comparison of the age of onset and the duration until the appearance of myoclonus and akinetic mutism from the onset between the rapid-type and the slow-type. The Grubbs-Smirnov critical test was used for statistical analysis of the duration until the appearance of PSWC from the onset between the rapid-type and the slow-type. Fisher's exact probability test was used for comparison of the male to female ratio, and the rates of myoclonus, akinetic mutism, and PSWC between the two types. It was also used for comparison of the positive rate of 14-3-3 immunoassay and MRI between the two types.

Results

Reviewing the clinical records of the enrolled patients, we found that no patients of either group had a family history of prion disease or dementia.

Fifteen patients, eight men and seven women, with a mean onset age of 65.4 ± 5.2 (Mean ± SD) years could be categorized as the rapid-type. Of those, seven with an initial symptom of progressive dementia or memory disturbance, two with visual symptoms, two with cerebellar ataxia, two with involuntary movement, and two with other symptoms. All except for one uncertain patient demonstrated myoclonus 2.4 ± 1.8 months after the onset. All became akinetic and mute within a mean duration of 3.1 ± 1.5 months, and demonstrated PSWC (Fig. 2A and B) within a mean duration of 2.8 ± 1.8 months. CJD-related high intensity lesions [11] were detected in eight of the nine patients examined by MRI. Similar to sCJD, three patterns existed: in one, high intensity lesions appeared mainly in the striatum (Fig. 3A); in another, they appeared in the striatum and the cortical ribbon equally (Fig. 3B); and in yet another, they appeared mainly in the cortical ribbon (Fig. 3C). The 14-3-3 protein assay was positive in all eight patients examined. All 15 patients showed MM129, 14 showed glutamic acid homozygosity at codon 219 (GG219) and one showed glutaminic acid/lysine heterozygosity at codon 219 in the PRNP analysis. These clinical features closely resembled typical sCJD with MM1 [3]. Immunohistochemical staining of PrP in four patients (one original patient and three previously reported patients [6]) revealed a diffuse synaptic-type deposit (Fig. 4A). The molecular type of PrP^{Sc} in one patient was type 1.

Five patients, two men and three women, with a mean onset age of 59.0 ± 12.8 years could be categorized as the slow-type. Three had an initial symptom of progressive dementia or memory disturbance, one showed psychiatric symptoms, and one had dressing apraxia. Four of five patients demonstrated myoclonus 15.3 ± 12.3 months after the onset, and the remaining one did not demonstrate myoclonus during the 13-month observation period. All became akinetic and mute within a mean duration of 20.6 ± 4.4 months. Only one demonstrated PSWC within the observation period of 23.8 ± 13.7 months (Fig. 2C and 2D). CJD-related high-intensity lesions were detected in four of the five patients examined by MRI [11]. One showed high-intensity lesions in the cortical ribbon (Fig. 3D and 3E), while in the others such lesions appeared in both the striatum and cortical ribbon (Fig. 3F). The medial thalami showed high-intensity lesions in all three patients examined by DWI (white arrows in Fig. 3D and E, and black arrows in Fig. 3F). The 14-3-3 protein assay was positive in all four patients examined. In the PRNP analysis, all five patients showed MM129 and GG219. Immunohistochemical staining in two patients revealed predominantly perivacuolar-type PrP deposits in the cerebral cortex (Fig. 4B), but also partly the diffuse synaptic-type deposits. In one patient, only the diffuse synaptic-type deposits were revealed. The molecular type of PrP^{Sc} in one patient who had predominantly perivacuolar-type PrP deposits was type 1 + 2.

Between the two groups, there were no differences in the age at onset, male to female ratio, or positive rate of

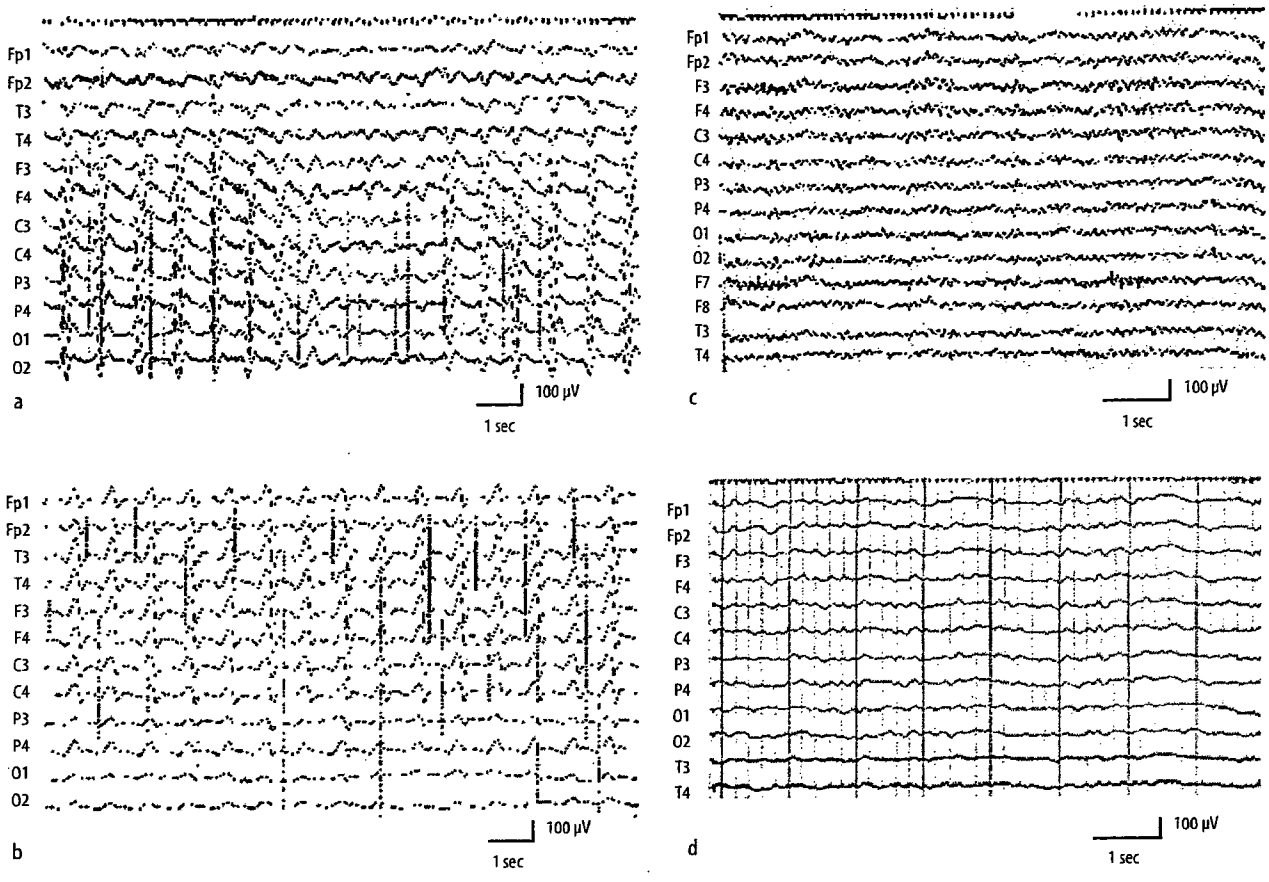

Fig. 2 EEG of representative patients of the rapid-type group and the slow-type group. **A** and **B** were recorded from the same 55-year-old woman in the rapid-type group. **C** and **D** were recorded from the same 69-year-old woman in the slow-type group. **A** EEG obtained two and half months after onset demonstrated high amplitude periodic sharp and wave complexes (PSWC) at a frequency of 1.5 Hz characteristic of CJD. **B** EEG obtained five months after the onset demonstrated PSWC at a frequency of 1 Hz. The amplitude was lower than that of Fig. 1A, and the background activities were flattened. EEG rapidly deteriorated. **C** EEG obtained four months after the onset. The background activities were 8 Hz mixed with no apparent slow activities. PSWC was not demonstrated. **D** EEG obtained twelve months after the onset. The background activities were 5 Hz mixed with δ activities. However, PSWC was not yet demonstrated

14-3-3 protein immunoassay. Similar to sCJD, there were three patterns of high-intensity lesions shown by MRI in the rapid-type. We were unable to distinguish the rapid-type of CJD232 from sCJD based on the clinical features including MRI findings. Patients with the slow-type did not have fewer lesions than patients with the rapid-type at diagnosis. High-intensity lesions in the medial thalamus depicted by DWI were a common finding of the slow-type (Fig. 3A–F). There was no difference in the rate of myoclonus between the two groups, but the duration until the appearance from the onset was longer in the slow-type compared with the rapid-type ($p < 0.005$). All patients became akinetic and mute in both types, but the duration until becoming akinetic and mute from the onset in the slow-type was longer than that in the rapid-type ($p < 0.001$). Concerning PSWC, all patients in the rapid-type demonstrated PSWC 2.8 ± 1.8 months after the onset. However, in the observation period of 21.6 ± 12.8 months, only one patient with the slow-type demonstrated PSWC 13 months after onset, which was later compared with that of the rapid-type ($p < 0.01$). The rate of PSWC in the slow-type was lower than that in the rapid-type ($p < 0.01$). Since there were no differences in the polymorphisms of codons 129 and 219 between the two groups, such polymorphisms would not be determinants of the disease subtype. Based on the differences in the clinical and laboratory findings (Table 1), we considered that these two types represented completely different phenotypes of exactly the same genotype.

By reviewing the investigative reports collected by the Creutzfeldt-Jakob Disease Surveillance Committee, Japan, as of February 2006, PRNP information was available from 511 patients: 317 were acknowledged as sporadic CJD, 41 as infectious CJD, 103 as genetic prion disease that included 28 CJD with V180I (CJD180), 27 GSS with P102L, 23 CJD with E200K, and 13 CJD232, and 50 as non-CJD. Three of the 50 non-CJD patients who had